Journal of the Korean Society for Nondestructive Testing
Vol. 26, No. 6 (2006. 12)

A Feasibility Study of Guided Wave Technique for Rail Monitoring

J.L. Rose*, C.M. Lee** and Y. Cho***,†

Abstract The critical subject of transverse crack detection in a rail head is treated in this paper. Conventional bulk wave ultrasonic techniques oftenfail because of shelling and other surface imperfections that shield the defects that lie below the shelling. A guided wave inspection technique is introduced here that can send ultrasonic energy along the rail under the shelling with a capability of finding the deleterious transverse crack defects. Dispersion curves are generated via a semi analytical finite element technique along with a hybrid guided wave finite element technique to explore the most suitable modes and frequencies for finding these defects. Sensor design and experimental feasibility experiments are also reported.

Keywords: Guided Wave, Rail Inspection

1. Introduction

The ultrasonic testing using guided wave is a very promising technique because the guided wave can propagate long distance along the structure. Practical applications of guided waves for pipes were performed by Rose et al., Lowe et al., and Alleyne and Cawley (Rose, et al., 1992; Rose, et al., 1994; Lowe et al., 1998; Alleyne and Cawley, 1997).

The applications to the rail are also carried out by Rose, Cawley, Cho and Hayashi (Lee et al., 2006a; Lee et al., 2006b; Rose et al., 2002a; Rose et al., 2002b; Cawley et al., 2003; Hayashi et al., 2003).

The numerous modes in a rail make it difficult to use of normal mode expansion technique in a practical testing. (Cho and Rose, 1996).

For this reason, a typical boundary value problem based on the wave mechanics is considered. The finite element technique is used to solve this boundary value problem. In the rail industry, the numerous types of defects can be located in a rail. The shelling defects are usually located above the transverse crack and make it difficult to fine the transverse crack with traditional technique using ultrasound.

2. Problem Statement

Because of the arbitrary shape of a cross-section of a rail, the phase velocity dispersion curves can be calculated with the semi-analytical finite element (SAFE) technique (Hayashi, et al., 2003).

Fig. 1 shows the phase velocity dispersion curves. It also displays the two calculation points where the wave scattering patterns are studied. The numerical model of the rail is modified to examine the influence of shelling. Initial

Received: October 24, 2006, Accepted: Novemver 25, 2006. * FBS Co., State College, Pennsylvania, USA, ** Ultrasonics R&D Lab., Engineering Science and Mechanics Dept., The Pennsylvania State University, USA, *** School of Mechanical Engineering, Pusan National University, Pusan, South Korea, † Corresponding author: mechcyh@pusan.ac.kr

geometries were taken from the report (FAR Research Report, 2003).

Fig. 2 shows the location and size of the defects and the shelling. The shapes of the defects are approximately rectangular with 0.1 mm crack width. These defects are started 4 mm under the top surface of the rail head. The half circle shaped shelling lies above the defect 1 mm below the top surface of the rail head.

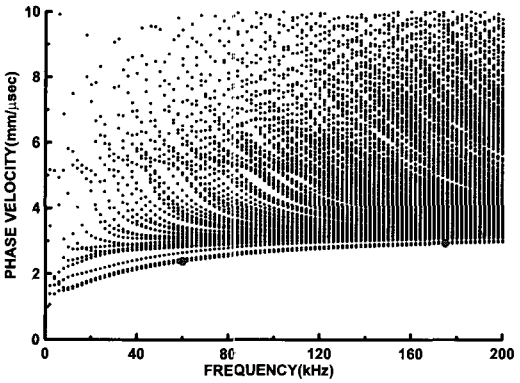

Fig. 1 Phase velocity dispersion curves of a rail

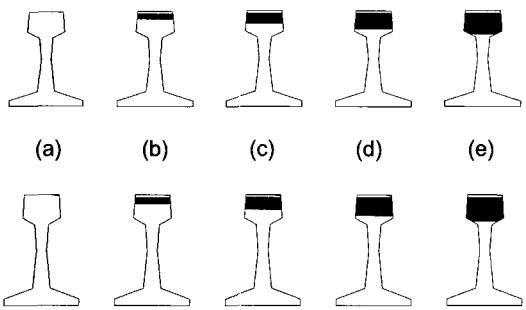

Fig. 2 Cross section of the rail with shelling and various defects
[(a): no defect, (b): 10 mm defect, (c): 20 mm defect, (d): 30 mm defect, (e): 40 mm defect, (f): shelling, (g): 10 mm defect with shelling, (h): 20 mm defect with shelling, (i): 30 mm defect with shelling, (j): 40 mm defect with shelling]

3. Wave Scattering from Defects

The Lamb type EMAT transducers are simulated with an input signal of 60 kHz and 175kHz. Fig. 3 shows the displacements of the reflected and transmitted waves at 185 mm from the defect without the shelling ((a)-(e) in Fig. 2) for the 60 kHz case. The reflected wave from the bigger defect has the larger displacement and the transmitted wave from the smaller defect has the larger displacement.

The reflected waves in Fig. 3 are separated from the incident wave. However, it is difficult to distinguish the incident wave and reflected wave at the closed position from the crack. On the contrary, the transmitted waves are relatively clear. For this reason, the maximum value of the absolute value of U2 (vertical displacement of the rail) at several points for 60 kHz and 175 kHz are plotted in Fig. 4 and Fig. 5 respectively.

In Fig. 4, the magnitudes of |U2| between 150 mm and 450 mm are monotonically decreased with the crack depth. However, the amplitudes of no defect and 10 mm defect with shelling are

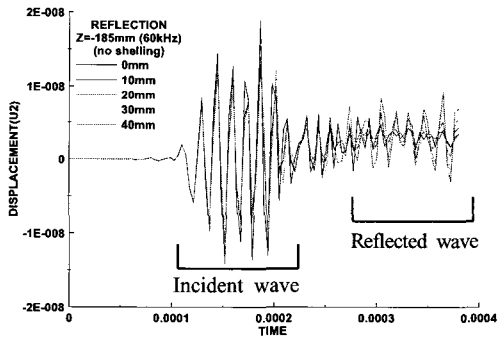

(a) Reflected waves

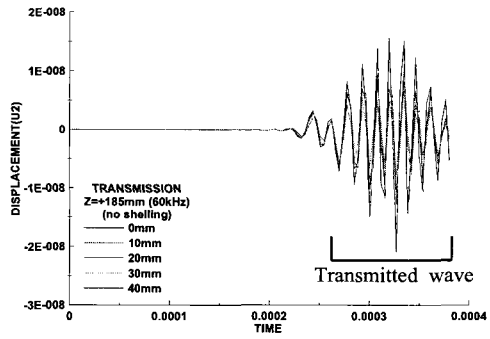

(b) Transmitted waves

Fig. 3 Reflected and transmitted waves at 185 mm from the defect without shelling (60 kHz)

almost the same, because the size of the crack is relatively small. As shown in Fig. 5 (a), the magnitude of |U2| between 100 mm and 200 mm shows a large difference between defects and no defect without shelling. On the contrary, the magnitude of |U2| in the same region shows no big difference between defects and no defect with shelling. Because the wave with higher frequency is closer to a surface wave and the shelling is treated as a defect.

4. Experimental Comfirmation

4.1 A Hole in a Clean Rail Head Surface

The experiments for various types of artificial defects were performed in the laboratory. To generate guided waves and to receive reflected waves from the defects, the lamb type EMATs with four different frequencies (60 kHz, 100 kHz, 185 kHz, and 280 kHz) were used in a pulse-echo mode. The first specimen is a rail with a 0.25" diameter hole and a clean rail head surface. Fig. 6 shows the location of a hole in the rail. Fig. 7 shows the position of the hole and the EMAT locations. The guided waves are generated from the transmitter, passing the receiver directly, propagating along the rail, and then reflected from a hole or a rail end, and then arriving at the receiver again. Signals were obtained at different distances from a hole by moving the transmitter and the receiver. Fig. 8 shows the RF waveform at 18" from a hole as an example.

Unlike the numerical experiments, a received

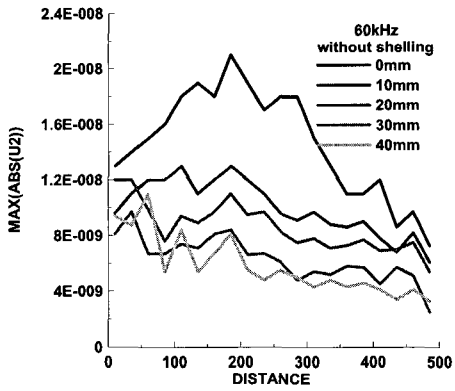

(a) |U2| without shelling

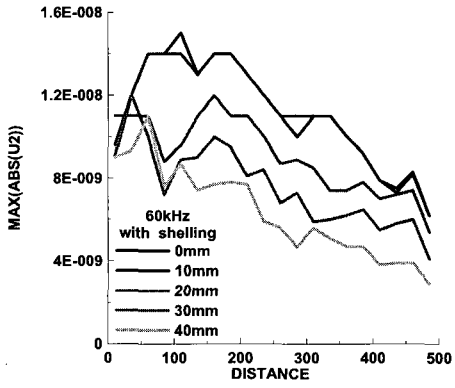

(b) |U2| with shelling

Fig. 4 Absolute value of U2 of the transmitted wave at several points (60 kHz)

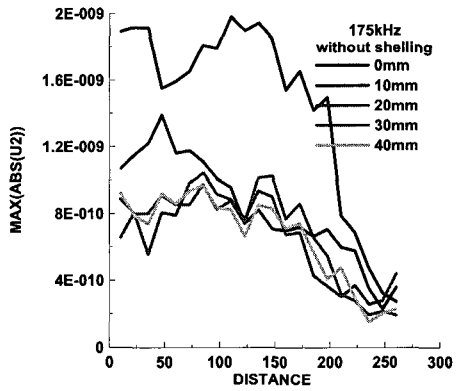

(a) |U2| without shelling

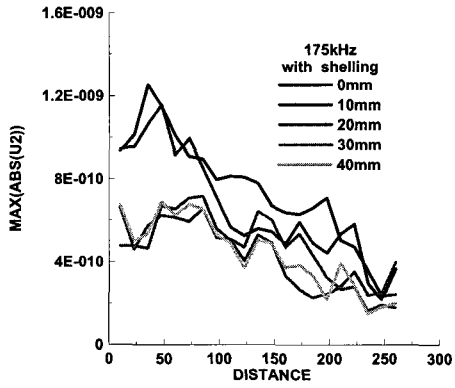

(b) |U2| with shelling

Fig. 5 Absolute value of U2 of the transmitted wave at several points (175 kHz)

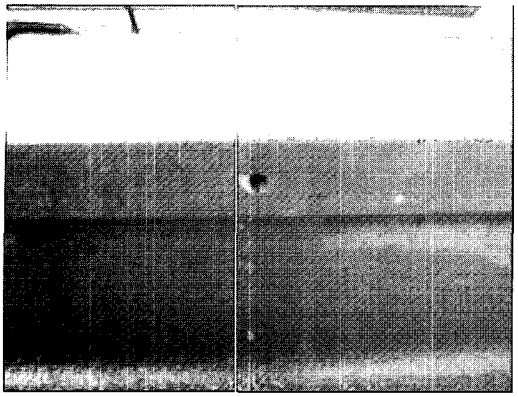

Fig. 6 A photograph of a hole in a clean rail

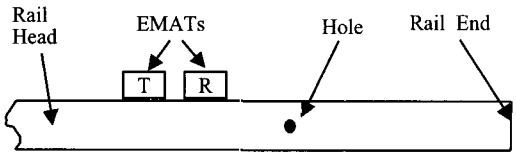

Fig. 7 The position of a hole and EMATs

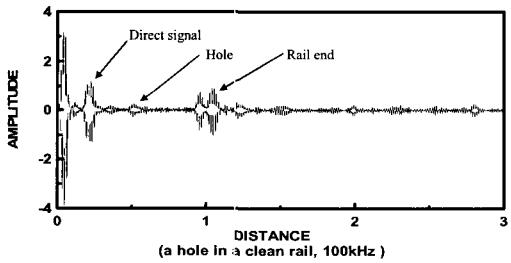

Fig. 8 RF wave form of a reflected wave from a hole in a clean rail for a 100 kHz guided wave at a distance of 0.45 m showing the direct signal, hole, and rail end.

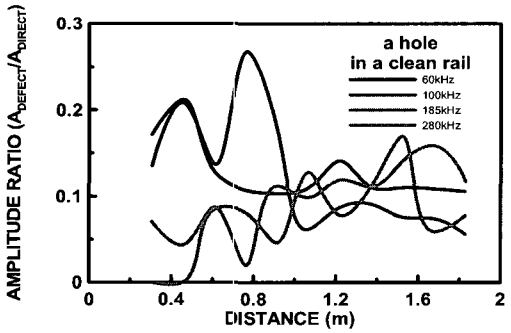

Fig. 9 Amplitude ratio for a rail with a clean surface of a rail head and a hole showing that at a distance less than 1m, 60 kHz and 100 kHz guided waves have more potential for detecting the hole

signal can be affected by many factors such as filtering, alignment of the EMATs, liftoff of the magnet of the EMAT, and the number of cycles used for input. Among them, the alignment of the EMATs is different when moved to new position. If the EMATs are misaligned, then both the direct signal and the reflected signal have small amplitudes. Therefore, the reflected signal from a defect is normalized with the direct signal. Fig. 9 shows the amplitude ratio of a reflected signal from a hole and a direct signal for a rail with a clean rail head surface with a hole at different positions. At a distance less than 1m, 60 kHz and 100 kHz guided waves have more potential for detecting the hole and after 1m, guided waves for four frequencies have a similar ability for detecting the hole.

4.2 A Hole in a Rough Rail Head Surface

The third specimen is a rail with a rough rail head surface and a 0.25" diameter hole. It is shown in Fig. 10. Fig. 11 shows the amplitude ratio for a rail with a rail head rough surface and a hole at different positions. In this case, the guided waves for 280 kHz cannot detect a hole over the entire distance since a collection of small echoes from the rough surface does not allow any energy to reach the defect. On the contrary, guided waves for lower frequencies (60 kHz and 100 kHz) can find the hole.

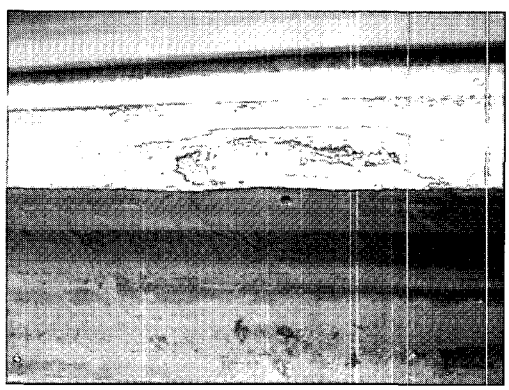

Fig. 10 A photograph of a hole in a rough rail

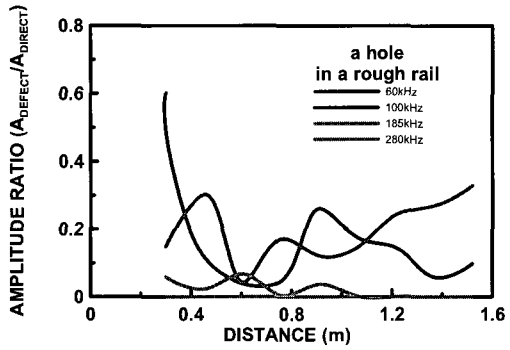

Fig. 11 Amplitude ratio for a rail with a rough rail head surface and a hole showing that guided waves for 60 kHz and 100 kHz can find the hole, 185 kHz is marginal, and the 280 kHz guided wave cannot see the hole since a collection of small echoes from the rough surface does not allow any energy to reach the defect

5. Conclusions

In this paper, the lamb type EMAT transducers are simulated using finite element technique. The characteristics of scattering from defects and shelling are also explored. The absolute values of U2 (vertical displacement of the rail) of transmitted waves are monotonically decreased with the crack depth for 60 kHz lamb wave. For 175 kHz lamb wave can not distinguish the shelling and the crack. The absolute values of U2 of transmitted waves show the big difference between defects without shelling and no defect without shelling for 175 kHz lamb waves.

The experiments for hole defect in a clean and rough rail were performed in the laboratory. To generate guided waves and to receive reflected waves from the defects, the lamb type EMATs with four different frequencies (60 kHz, 100 kHz, 185 kHz, and 280 kHz) were used in a pulse-echo mode. The guided waves with higher frequency (185 kHz and 280 kHz) are sensitive to the surface roughness of the rail head because the most of energy is concentrated in the top surface of the rail head.

Therefore, the best condition in detecting a transverse defect under a shelling is the guided waves with lower frequencies (60 kHz and 100 kHz).

Acknowledgement

Thanks are given to Pusan National University and the Federal Railroad Administration for the support in the period from 2004 to 2006. Thanks are also given to Mike Avioli at FBS. Inc. for his assistance.

References

Alleyne, D. N. and Cawley, P. (1997) Long Range Propagation of Lamb Waves in Chemical Plant Pipe Work, *Materials Evaluation*, Vol. 55, pp. 504-508

Cawley, P., Lowe, M. J. S., Alleyne, D. N., Pavlakovic B. and Wilcox, P. (2003) Practical Long Range Guided Wave Testing : Application to Pipes and Rails, *Materials Evaluation*, Vol. 61, No. 1, pp. 66-74

Cho, Y. and Rose, J. L., (1996) A Boundary Element Solution for a Mode Conversion Study on the Edge Reflection of Lamb Waves, *J. Acoust. Soc. Am.* Vol. 99, No. 4, pp. 2097-2109

Flaw Characterization of Rail Service Failures, Report No. R-963 AAR Research Report (2003)

Hayashi, T., Song, W. J. and Rose, J. L. (2003) Guided Wave Dispersion Curves for a Bar with an Arbitrary Cross-Section, a Rod and Rail Example, *Ultrasonics*, Vol. 41, pp. 175-183

Lee, C. M., Rose, J. L., Luo, W. and Cho, Y. (2006) A Computational Tool for Defect Analysis in Rail with Ultrasonic Guided Waves, *Key Engineering Materials*, Vols. 321-323, pp. 784-787

Lee, C. M., Rose, J. L.., and Cho, Y. (2006)

A Characteristic of Scattering Patterns from Defect in a Rail,, *Key Engineering Materials*, Vols. 321-323, pp. 788-791

Lowe, M. J. S., Alleyne, D. N. and Cawley, P. (1998) The Mode Conversion of a Guided Wave by a Part-Circumferential Notch in a Pipe, *J. Appl. Mech.*, Vol. 65, pp. 211-214

Rose, J. L., Ditri, J. J., Pilarski, A., Zhang, Carr, J. F. T. and McNight, W. J. (1992) A Guided Wave Inspection Technique for Nuclear Steam Generator Tubing, *Nondestr. Test.* Vol. 92, pp. 191-195

Rose, J. L., Rajana, K. M. and Carr, F. T. (1994) Ultrasonic Guided Wave Inspection Concepts for Steam Generator Tubing, *Mater. Eval.*, Vol. 52, No. 2, pp. 307-311

Rose, J. L., Avioli M. J. and Song, W. J. (2002) Application and Potential of Guided Wave Rail Inspection, *Insight*, Vol. 44, No. 6, pp. 353-358

Rose, J. L., Avioli, M. J. and Cho, Y. (2002) Elastic Wave Analysis for Broken Rail Detection, *Review of Quantitative Nondestructive Evaluation*, Vol. 21, pp. 1806-1812